Statistics of chaotic resonances in an optical microcavity

Li Wang,[1] Domenico Lippolis,[2,3] Ze-Yang Li,[1] Xue-Feng Jiang,[1] Qihuang Gong,[1] and Yun-Feng Xiao[1,*]

[1]*State Key Laboratory for Mesoscopic Physics and School of Physics, Peking University;*
Collaborative Innovation Center of Quantum Matter, Beijing 100871, China
[2]*Institute for Advanced Study, Tsinghua University, Beijing 100084, China*
[3]*Faculty of Science, Jiangsu University, Zhenjiang 212013, China*

Distributions of eigenmodes are widely concerned in both bounded and open systems. In the realm of chaos, counting resonances can characterize the underlying dynamics (regular vs chaotic), and is often instrumental to identify classical-to-quantum correspondence. Here, we study, both theoretically and experimentally, the statistics of chaotic resonances in an optical microcavity with a mixed phase space of both regular and chaotic dynamics. Information on the number of chaotic modes is extracted by counting regular modes, which couple to the former via dynamical tunneling. The experimental data are in agreement with a known semiclassical prediction for the dependence of the number of chaotic resonances on the number of open channels, while they deviate significantly from a purely random-matrix-theory-based treatment, in general. We ascribe this result to the ballistic decay of the rays, which occurs within Ehrenfest time, and importantly, within the time scale of transient chaos. The present approach may provide a general tool for the statistical analysis of chaotic resonances in open systems.

Introduction. The statistics of chaotic resonances has been a central topic of theoretical and experimental interest for decades [1–8], as a doorway to better understand chaotic scattering in quantum mechanics [9–12]. Counting chaotic resonances notably finds applications in optical resonators [13–15], where chaos can be used, for example, to enhance energy storage [16] or enhance coupling [17,18]. In the realm of fundamental problems, an estimate of the number of states within a certain frequency interval is given by the fractal Weyl law [19–23]. Predicted more than a decade ago, this theory is still awaiting experimental confirmation at optical frequencies. The delay is mainly due to two obstacles: (i) the theoretical problem of accounting for partial absorption [24,25]; and (ii) the experimental challenge of analyzing overlapping resonances [26]. By introducing methods to overcome these hurdles, we theoretically and experimentally study the statistics of chaotic resonances in two-dimensional asymmetric optical microcavities, and thus present a significant result in the context of fractal Weyl laws at optical frequencies. An absorber is placed underneath the microcavity appositely to realize a virtually full opening, and therefore solve the problem of partial absorption. In order to handle overlapping resonances, we exploit the mixed classical phase space of the present cavity, and exclusively count high-Q regular modes, easily recognized in the measured spectra due to their narrow linewidths, and that enables us to draw information on the low-Q chaotic modes, coupled to the regular ones via dynamical tunneling [27].

Theoretical model. The dynamics inside the cavity is described by a non-Hermitian Hamiltonian $H = H_0 + V$, where H_0 has eigenstates $|C_\omega\rangle$ (regular) and $|C_n\rangle$ (chaotic), while V represents the coupling between them [28,29]. Following a standard approach [30,31], the electromagnetic field excited by the incident beam can be written as a superposition of one regular and several chaotic modes,

$\psi(x,t) = a_\omega(t)c_\omega(x)e^{-i\omega t} + \sum_n b_n(t)c_n(x)e^{-i\omega_n t}$. The a_ω and b_n are oscillator amplitudes driven by the laser beam, coupled to each other with strength V_n (real), with damping rates γ_ω and γ_n, respectively. Then, in the overdamped regime ($|V_n| \ll \gamma_n$), the dynamical equations for the time-dependent envelopes take the form [17]

$$\dot{b}_n + \gamma_n b_n = f_n E_0 - V_n a_\omega, \qquad (1a)$$

$$\dot{a}_\omega + [\gamma_\omega + i(\omega_0 - \omega)]a_\omega = \sum_n V_n b_n, \qquad (1b)$$

where f_n is the coupling strength of the nth chaotic mode with the laser beam of amplitude E_0 and frequency ω_0. We are interested in the steady-state solution, obtained by setting $\dot{a}_\omega = \dot{b}_n = 0$. The amplitude a_ω of the envelope of the regular mode is then found to be

$$a_\omega = \frac{E_0 \sum_n f_n \frac{V_n}{\gamma_n}}{[\gamma_\omega + i(\omega - \omega_0)] + \sum_n \frac{V_n^2}{\gamma_n}}. \qquad (2)$$

We only sum over n_γ chaotic modes with linewidth smaller than a certain value set by γ, and use the averages $\bar{f}, \bar{V}, \bar{\gamma}$ to approximate the summations as $\sum_n f_n \frac{V_n}{\gamma_n} \sim n_\gamma \frac{\bar{f}\bar{V}}{\bar{\gamma}}$, $\sum_n \frac{V_n^2}{\gamma_n} \sim n_\gamma \frac{\bar{V}^2}{\bar{\gamma}}$ [32]. The result is, at resonance ($\omega = \omega_0$),

$$|a_\omega|^2 = \epsilon^2 \frac{n_\gamma^2}{\Gamma^2 + n_\gamma^2}, \qquad (3)$$

where $\epsilon = E_0 \bar{f}/\bar{V}$, and $\Gamma = \gamma_\omega \bar{\gamma}/\bar{V}^2$.

Equation (3) is central to the present work, as it bridges between the number of excited regular modes (proportional to $|a_\omega|^2$), which we measure directly, and the number of chaotic modes n_γ, which we estimate. In the spirit of Weyl law, we test the prediction [33]

$$n_{\gamma,\mathrm{Weyl}} = M N^{-1/\mu\tau_d} \left[1 - \frac{1}{\tau_d} \frac{1}{1 - e^{-\gamma}} \right], \qquad (4)$$
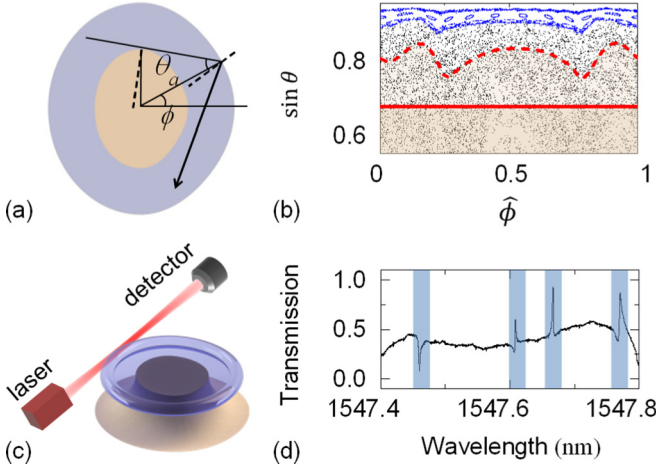
---

*yfxiao@pku.edu.cn; URL: www.phy.pku.edu.cn/~yfxiao/

FIG. 1. (a) Sketch of the deformed microcavity with an inner absorber, characterized by the angle θ_a. (b) Poincaré surface of section of the microcavity ($\hat{\phi} \equiv \phi/2\pi$) with deformation factor $\eta = 11.7\%$. Blue orbits are regular, black are chaotic. The red solid line indicates the angle of total internal reflection, while the dashed curve is given by an absorption angle such that $r \simeq 0.77$. Different shades of color indicate loss to the absorber (lighter) and by refraction into air (darker). (c) Schematic representation of the free-space coupled cavity system. (d) A typical transmission spectrum with the high-Q regular modes highlighted.

for the dependence of n_γ on the number of open channels N. Here M is the total number of chaotic states, $\tau_d = M/N$ is the mean dwelling time of a ray in the cavity, and μ is of the order of the Lyapunov exponent of the chaotic dynamics [32]. We focus on the role of the prefactor $N^{-1/\mu\tau_d}$, which accounts for the instantaneous-decay modes escaping from the system within the Ehrenfest time of quantum-to-classical correspondence [34]. By removing the prefactor, the remainder of Eq. (4) is solely based on random matrix theory (RMT) [35], and will also be tested against the observations.

Absorber in the optical cavity. In order to achieve the full opening required to test these predictions, we introduce an absorber in the cavity. In the analysis, the dielectric microcavity [Fig. 1(a)] has the deformed circle $\rho(\phi)$ as boundary [32], and encloses an absorber of shape $\rho(\phi) - R$. Figure 1(b) shows the classical phase space, together with the critical line of total internal reflection ($\sin\theta_c$), as well as the line given by the incidence angle θ_a, below which the reflected ray hits the absorber [36]. We assume that the rays hitting the absorber are completely absorbed. The rays that escape the cavity by refraction into the air with an angle of incidence $\theta \ll \theta_c$ are very lossy and, as such, they are not expected to contribute to the excitation of the regular modes, consistently with Eqs. (2) and (3). For that reason, we only take into account the states supported on a strip of the chaotic phase space with momentum above a certain threshold, $\sin\theta > \sin\theta_{th}$, to be chosen below but close enough to the critical line of total internal reflection. Let us introduce the notation $\xi \equiv \sin\theta_a - \sin\theta_{th}$ to indicate the strip of the phase space opened by the absorber. Using the picture of Ref. [33], there are effectively N open channels out of the M Planck cells available in the phase space, produced by the absorber
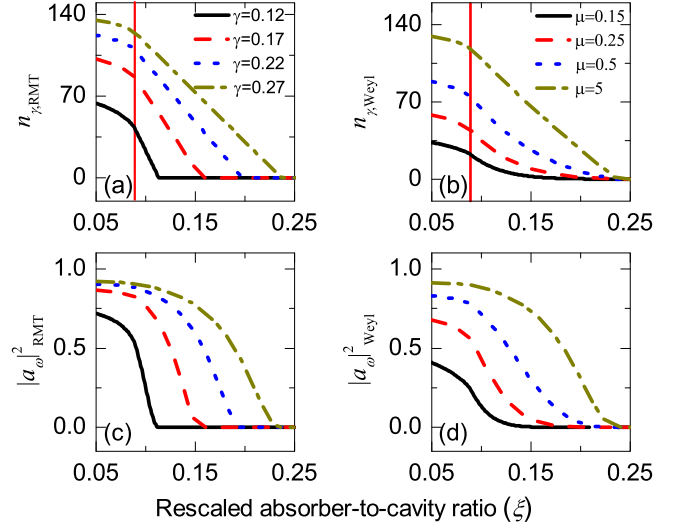

FIG. 2. (a), (b) Number of chaotic states n_γ vs the rescaled absorber-to-cavity ratio ξ, obtained by RMT and Weyl law, respectively. (c), (d) The corresponding expectations for $|a_\omega|^2$. In (d), the smaller μ, the more visible the tail of the excitation probability. The red vertical line corresponds to the critical angle, $\sin\theta_c \simeq 0.69$. Here $\sin\theta_{th} = 0.6$.

(full opening, N_a) and the refraction out of the cavity (partial opening, N_r), so that the mean dwelling time of a ray is given by

$$\tau_d = \frac{M}{N_a + N_r}, \tag{5}$$

with $N_r = \frac{M}{A} \int_{\sin\theta_a}^{\sin\theta_c} d\sin\theta\, T(\sin\theta)$, T transmission coefficient according to Fresnel law, and A area of the phase space in exam, while $N_a = M\xi/A$.

Recalling the original purpose of studying the statistics of chaotic resonances, we proceed by steps and first examine the RMT-based prediction $n_{\gamma,\mathrm{RMT}} = M[1 - \frac{1}{\tau_d}\frac{1}{1-e^{-\gamma}}]$, rewritten as (set $\hat{\xi} = 1/\tau_d = \xi/A + N_r/M$)

$$n_{\gamma,\mathrm{RMT}} = M\left[1 - \frac{\hat{\xi}}{1 - e^{-\gamma}}\right]. \tag{6}$$

The theoretical expectation is portrayed in Fig. 2(a): $n_{\gamma,\mathrm{RMT}}$ changes relatively slowly for ξ small such that $\theta_a < \theta_c$, when the loss is mainly due to refraction into air. Otherwise $n_{\gamma,\mathrm{RMT}}$ decreases more rapidly and linearly with ξ in the region of total internal reflection, when the loss is entirely due to the absorber. Plugging Eq. (6) into Eq. (3), the probability of excitation of the high-Q regular modes $|a_\omega|^2_{\mathrm{RMT}}$ starts to fall off only when ξ reaches some critical value, controlled by the parameter γ [Fig. 2(c)]. The other parameter $\tilde{\Gamma} = \gamma_\omega \bar{\gamma}/M\bar{V}^2$ controls the slope of the curve. It is noted that the probability of excitation of the regular modes decreases dramatically when the loss is entirely due to the absorber, in which case the system is fully open.

On the other hand, the semiclassical estimate (4) becomes, as a function of $\hat{\xi}$,

$$n_{\gamma,\mathrm{Weyl}} = \frac{M^{1-\hat{\xi}/\mu}}{\hat{\xi}^{\hat{\xi}/\mu}}\left[1 - \frac{\hat{\xi}}{1 - e^{-\gamma}}\right]. \tag{7}$$

The quantity μ, of the order of the Lyapunov exponent of the chaotic region of the phase space [32], is what really characterizes (7), which resembles the linear RMT prediction (6) for large enough μ, and otherwise becomes visibly nonlinear [Figs. 2(a) and 2(b)] when $\mu \ll 1$. This nonlinearity produces a *characteristic tail* in the curve expressed by Eq. (3) [Fig. 2(d)], meaning that the effect of the Ehrenfest time scale on the excitation of the regular modes is most evident slightly above the onset of chaos.

Experimental setup and measurement. The experimental apparatus consists of a deformed toroidal microcavity [18] coupled to a laser beam (of wavelength $\lambda \simeq 1550$ or 635 nm), as shown in Fig. 1(c). The microtoroid (refractive index $\simeq 1.44, 1.46$ depending on λ) has principal (minor) diameters of 120 μm (5 μm), consistently with the two-dimensional model [32]. Thus the effective Planck constant $h_{\text{eff}} \sim \lambda/a \sim 10^{-2}$ (a: principal diameter) justifies the semiclassical analysis. The microcavity is fabricated through optical lithography, buffered HF wet etching, XeF_2 gas etching, and CO_2 pulse laser irradiation. The resulting silica microtoroid is supported by a silicon pillar of similar shape, which has a high refractive index ($\simeq 3.48, 3.88$), and it acts as the absorber in the model. After each measurement of the free-space transmission spectrum [Fig. 1(d)], the top diameter of the silicon pillar, connected with the silica disk, is progressively reduced by a new isotropic XeF_2 dry etching process. In this way we control the openness of the microcavity with the ratio r between the top diameters of pillar and toroid. Finite element method simulations show that the light power decreases to less than 5% of the input value, when propagating by a distance of 20 μm inside the 2-μm-thick silica waveguide bonding with a silicon wafer [32], as is reasonable to expect, given the high refractive index of the silicon. Thus the silicon pillar acts as a full absorber, consistently with the present model. On the other hand, high-Q regular modes living inside the toroidal part, whose cross section has minor diameter of 5μm, do not leak into the silicon pillar and therefore are not directly affected by the pillar size [32]. The dependence of the free-space transmission spectra on the pillar size is shown in Fig. 3. When the pillar approaches the inner edge of the toroid [Figs. 3(a) and 3(e), $r \simeq 0.81$], no high-Q regular modes are observed in the spectrum, since most of the probe laser field in the cavity radiates into the silicon and cannot tunnel to high-Q regular modes. As we gradually reduce the size of the pillar [Fig. 3(f), $r \simeq 0.77$], increasingly many high-Q modes appear in the spectrum [Fig. 3(b)]. When the absorber-to-cavity ratio r is small enough [Figs. 3(g) and 3(h), $r \lesssim 0.7$], the transmission no longer changes sensibly [Figs. 3(c) and 3(d)], and the number of high-Q modes in the spectrum also stabilizes.

Statistics of chaotic resonances. As anticipated, we use the transmission spectra to test the theory, by counting the excited high-Q regular modes for different sizes of the silicon pillar [37]. The results are illustrated in Fig. 4, for two microcavities of distinct deformations. In the RMT-based approach [Eqs. (3) and (6)] we have two fitting parameters, γ and $\tilde{\Gamma}$, while the total number of chaotic states is estimated theoretically as $M \simeq A/h_{\text{eff}}$ (A area of the phase space we consider). Figure 4(a) shows overall agreement between the experimental data (dots) and this theory (blue dashed curve), which however deviates from the tail visible at larger sizes
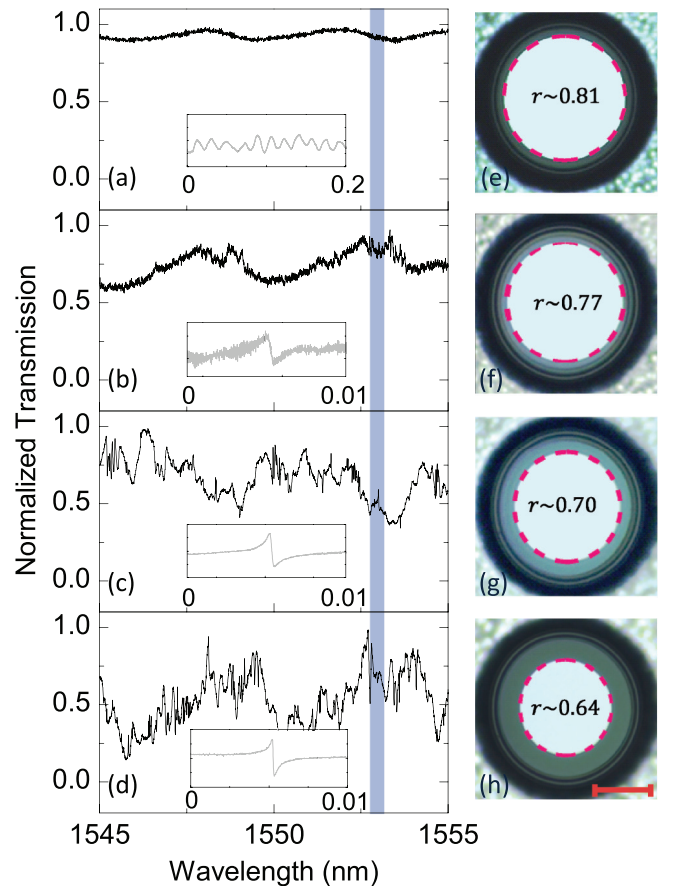

FIG. 3. Normalized transmission and top-view optical images of the cavity with $r \simeq 0.81$ [(a) and (e)], 0.77 [(b) and (f)], 0.70 [(c) and (g)], and 0.64 [(d) and (h)]. Inset of (a) shows background noise. Insets of (b)–(d) show the high-Q modes. Reflection of the silica-to-silicon interface results in a brighter color for the silicon pillar in the optical image (boundary shown by red dashed curves). Scale bar is 50 μm.

of the absorber. The discrepancy becomes more apparent for the cavity with a lower deformation factor η [Fig. 4(b)]. A quantitative test of the goodness of the fit yields a reduced $\chi^2 \simeq 1.7, 5.6$ for $\eta \simeq 11.7\%, 6\%$, respectively [32,38], the latter deviating significantly from the optimal value of unity.
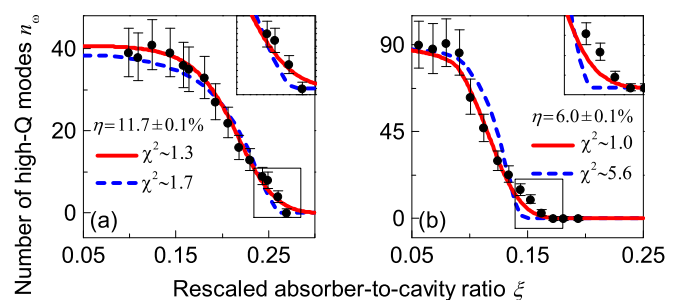

FIG. 4. (a), (b) Number of high-Q regular modes (n_ω) observed experimentally in the microcavities of $\eta = 11.7\%$ and 6%, respectively, vs rescaled absorber-to-cavity ratio ξ. Blue dashed and red solid curves are, respectively, RMT and Weyl-law best fits, whose goodness is assessed by χ^2. Here $\sin \theta_c \simeq 0.69$ and $\sin \theta_{\text{th}} = 0.6$. Inset: area where the two curves differ most.

The fitted maximum escape rate $\gamma \simeq 0.2, 0.3$ is the inverse (in units of Poincaré time) of the minimum escape time τ_{esc} of the chaotic rays contributing to the excitation of the regular modes, from which $Q = 2\pi \nu \tau_{esc} \sim 10^3$, on average ($\nu$ is the frequency of the laser beam). We find this estimate consistent with the typical order of Q independently obtained from ray-dynamics simulations [32], which suggests the fitted parameter makes physical sense.

Next, we test the semiclassical correction (7), using the finite time Lyapunov exponent μ evaluated by direct iteration [32,39], with the estimated parameter M and the fitted parameters γ and Γ. It is found that the semiclassical correction (red solid curves) fits the experimental data better than the RMT-based estimate, especially at the smaller deformation, where the two predictions differ the most due to the smaller μ (cf. Fig. 2). Here $\chi^2 \simeq 1.3, 1$, indicating good agreement. In particular, we are now able to account for the tail of the curve, which corresponds to the microcavity having the largest openings and thus with the maximum number of instantaneous decay states, where the semiclassical correction is decisive. More experimental and fitting results at different wavelengths and deformations support the above explanation [32].

Conclusion and discussion. Let us summarize the work done and the results obtained. By counting the high-Q regular modes excited via dynamical tunneling as a function of the number of open channels, we have studied the statistics of the chaotic resonances in a dielectric microcavity with a full absorber. As main result, the experimental data deviate from a purely RMT-based prediction, while they exhibit better agreement with a semiclassical expression that factors out the number of instantaneous decay modes. Importantly, the latter estimate depends on the Lyapunov exponent of the chaotic dynamics, and it accounts for a characteristic tail in the decay of the number of regular modes, which we interpret as a signature of the ballistic escape of the rays into the absorber, occurring within Ehrenfest time.

Although the theoretical analysis does not take into account either partial transport barriers [40,41], or the "sticky" dynamics at the regular-chaotic border [20,21], which all cause long-time correlations to decay algebraically rather than exponentially, we argue in what follows that the current model is suitable for the resolution of our experiment. Figure 5 illustrates the survival probability in the chaotic region, obtained from extensive ray-dynamics simulations of
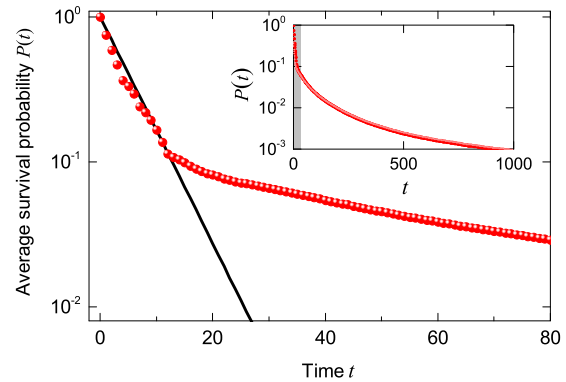

FIG. 5. Survival probability in the chaotic region (logarithmic scale). Points: average survival probability $P(t)$ of a ray in the microcavity vs t (in units of Poincaré time) at $\eta = 11.7\%$, $\xi = 0.13$, from 10^6 randomly started trajectories. Line: $P(t) = \exp(-t/\tau_d)$, $\tau_d = 6$. Inset: the long-time simulation showing algebraic decay.

the microcavity-shaped billiard: despite an overall power-law decay, a closer look at the short-time dynamics reveals that the decay is initially exponential, behavior known as transient chaos [42]. The estimates for the dwelling time τ_d, and the experimental values of γ, maximum decay rate of the chaotic resonances, are both within the time scale of exponential decay. That suggests that the suppression by the absorber of the longest-lived resonances (that scale algebraically with γ [21]) alone does not affect the number of excited WGMs measured in the experiment, and therefore is not detected by the current apparatus.

[1] C. Ellegaard, T. Guhr, K. Lindemann, J. Nygård, and M. Oxborrow, Symmetry Breaking and Spectral Statistics of Acoustic Resonances in Quartz Blocks, Phys. Rev. Lett. **77**, 4918 (1996).

[2] G. E. Mitchell, A. Richter, and H. A. Weidenmüller, Random matrices and chaos in nuclear physics: Nuclear reactions, Rev. Mod. Phys. **82**, 2845 (2010).

[3] A. Frisch, M. Mark, K. Aikawa, F. Ferlaino, J. L. Bohn, C. Makrides, A. Petrov, and S. Kotochigova, Quantum chaos in ultracold collisions of gas-phase erbium atoms, Nature (London) **507**, 475 (2014).

[4] P. Carpena, P. Bernaola-Galvàn, P. Ch. Ivanov, and H. E. Stanley, Metal-insulator transition in chains with correlated disorder, Nature (London) **418**, 955 (2002).

[5] H. Cao and J. Wiersig, Dielectric microcavities: Model systems for wave chaos and non-Hermitian physics, Rev. Mod. Phys. **87**, 61 (2015).

[6] K. Pance, W. Lu, and S. Sridhar, Quantum Fingerprints of Classical Ruelle-Pollicott Resonances, Phys. Rev. Lett. **85**, 2737 (2000).

[7] A. Wirzba, Quantum mechanics and semiclassics of hyperbolic n-disk scattering systems, Phys. Rep. **309**, 1 (1999).

[8] J. A. Folk, S. R. Patel, S. F. Godijn, A. G. Huibers, S. M. Cronenwett, C. M. Marcus, K. Kampman, and A. C. Gossard, Statistics and Parametric Correlations of Coulomb Blockade Peak Fluctuations in Quantum Dots, Phys. Rev. Lett. **76**, 1699 (1996).

[9] M. V. Berry and M. Robnik, Semiclassical level spacings when regular and chaotic orbits coexist, J. Phys. A **17**, 2413 (1984).

[10] P. Gaspard and S. A. Rice, Semiclassical quantization of the scattering from a classically chaotic repellor, J. Chem. Phys. **90**, 2242 (1989).

[11] P. So, S. M. Anlage, E. Ott, and R. N. Oerter, Wave Chaos Experiments with and without Time Reversal Symmetry: GUE and GOE Statistics, Phys. Rev. Lett. **74**, 2662 (1995)

[12] E. N. Pozzo, D. Domínguez, and M. J. Sánchez, Quantum chaos in the mesoscopic device for the Josephson flux qubit, Phys. Rev. B **77**, 024518 (2008).

[13] O. A. Starykh, P. R. J. Jacquod, E. E. Narimanov, and A. D. Stone, Signature of dynamical localization in the resonance width distribution of wave-chaotic dielectric cavities, Phys. Rev. E **62**, 2078 (2000).

[14] G. Hackenbroich, Statistical theory of multimode random lasers, J. Phys. A **38**, 10537 (2005).

[15] H. Schomerus, J. Wiersig, and J. Main, Lifetime statistics in chaotic dielectric microresonators, Phys. Rev. A **79**, 053806 (2009).

[16] C. Liu, A. D. Falco, D. Molinari, Y. Khan, B. S. Ooi, T. F. Krauss, and A. Fratalocchi, Enhanced energy storage in chaotic optical resonators, Nat. Photonics **7**, 473 (2013).

[17] J. Yang, S.-B. Lee, S. Moon, S.-Y. Lee, S. W. Kim, T. T. A. Dao, J.-H. Lee, and K. An, Pump-Induced Dynamical Tunneling in a Deformed Microcavity Laser, Phys. Rev. Lett. **104**, 243601 (2010).

[18] Y.-F. Xiao, X.-F. Jiang, Q.-F. Yang, L. Wang, K. Shi, Y. Li, and Q. Gong, Tunneling-induced transparency in a chaotic microcavity, Laser Photonics Rev. **7**, L51 (2013).

[19] W. T. Lu, S. Sridhar, and M. Zworski, Fractal Weyl Laws for Chaotic Open Systems, Phys. Rev. Lett. **91**, 154101 (2003).

[20] M. J. Körber, M. Michler, A. Bäcker, and R. Ketzmerick, Hierarchical Fractal Weyl Laws for Chaotic Resonance States in Open Mixed Systems, Phys. Rev. Lett. **111**, 114102 (2013).

[21] A. Ishii, A. Akaishi, A. Shudo, and H. Schomerus, Weyl law for open systems with sharply divided mixed phase space, Phys. Rev. E **85**, 046203 (2012).

[22] A. Potzuweit, T. Weich, S. Barkhofen, U. Kuhl, H.-J. Stöckmann, and M. Zworski, Weyl asymptotics: From closed to open systems, Phys. Rev. E **86**, 066205 (2012).

[23] S. Barkhofen, T. Weich, A. Potzuweit, H.-J. Stöckmann, U. Kuhl, and M. Zworski, Experimental Observation of the Spectral Gap in Microwave n-Disk Systems, Phys. Rev. Lett. **110**, 164102 (2013).

[24] S. Nonnenmacher and E. Schenck, Resonance distribution in open quantum chaotic systems, Phys. Rev. E **78**, 045202 (2008).

[25] M. Schönwetter and E. G. Altmann, Quantum signatures of classical multifractal measures, Phys. Rev. E **91**, 012919 (2015).

[26] J. Wiersig and J. Main, Fractal Weyl law for chaotic microcavities: Fresnel's laws imply multifractal scattering, Phys. Rev. E **77**, 036205 (2008).

[27] M. J. Davis and E. J. Heller, Quantum dynamical tunneling in bound states, J. Chem. Phys **75**, 246 (1981).

[28] O. Bohigas, S. Tomsovic, and D. Ullmo, Manifestations of classical phase space structures in quantum mechanics, Phys. Rep. **223**, 43 (1993).

[29] A. Bäcker, R. Ketzmerick, S. Löck, and L. Schilling, Regular-to-Chaotic Tunneling Rates using a Fictitious Integrable System, Phys. Rev. Lett. **100**, 104101 (2008).

[30] U. Fano, Effects of configuration interaction on intensities and phase shifts, Phys. Rev **124**, 1866 (1961).

[31] K. An and J. Yang, Mode-mode coupling theory of resonant pumping via dynamical tunneling processes in a deformed microcavity, in *Trends in Nano- and Micro-Cavities* (Bentham Science, Sharjah, U.A.E., 2011), pp. 40–61.

[32] See Supplemental Material at http://link.aps.org/supplemental/10.1103/PhysRevE.93.040201 for details.

[33] H. Schomerus and J. Tworzydlo, Quantum-to-Classical Crossover of Quasibound States in Open Quantum Systems, Phys. Rev. Lett. **93**, 154102 (2004).

[34] H. Schomerus and P. Jacquod, Quantum-to-classical correspondence in open chaotic systems, J. Phys. A **38**, 10663 (2005).

[35] K. Zyczkowski and H. J. Sommers, Truncations of random unitary matrices, J. Phys. A **33**, 2045 (2000).

[36] In what follows we neglect the dependence of θ_a on ϕ by taking the average value, which is determined by the ratio r of the mean radius of the absorber to the cavity's.

[37] Since we do not have an estimate for the parameter ϵ, all the data sets are fitted up to a multiplicative constant.

[38] J. R. Taylor, *An Introduction to Error Analysis* (University Science Books, Sauselito, CA, 1997).

[39] μ is computed over a short enough time for the dynamics to be still hyperbolic.

[40] J. Meiss, Symplectic maps, variational principles, and transport, Rev. Mod. Phys. **64**, 795 (1992).

[41] M. Michler, A. Bäcker, R. Ketzmerick, H.-J. Stöckmann, and S. Tomsovic, Universal Quantum Localizing Transition of a Partial Barrier in a Chaotic Sea, Phys. Rev. Lett. **109**, 234101 (2012).

[42] Y. C. Lai and T. Tél, *Transient Chaos* (Springer, New York, 2010).